Review Paper

Stabilizing and Destabilizing Effect of Shear Flow — Beyond Kelvin-Helmholtz Instability —

TATSUNO Tomoya*

Graduate School of Frontier Sciences, The University of Tokyo, Tokyo 113-0033, Japan

(Received 27 January 2003 / Accepted 11 August 2003)

Abstract

Recent progress in linear spectral studies of incompressible plasma (fluid) with flows is reviewed. Mathematically, non-Hermiticity of the generating operator brings about incompleteness of the eigenvalue analysis and unremovable coupling between modes. This may lead to secular growth (algebraic in time) even if all eigenvalues exhibit stable oscillations. Physically, the stretching effect of shear flow is considered a stabilizing mechanism for various plasma instabilities; however, shear flow may equally effectively destabilize a class of plasma modes. The condition for stabilization/destabilization is discussed as well as its physical mechanisms.

Keywords:

linear stability, shear flow, stretching effect, Non-Hermiticity (non-self-adjointness), nilpotent, Kelvin-Helmholtz instability, Alfvén wave

1. Introduction

Shear flows in plasmas are attracting much interest because of their suppression effect on turbulence in magnetically confined fusion devices. The current naïve suggestion regarding this phenomena holds that the stretching of modes in a shear flow brings about length scale reduction leading to the suppression of fluctuations. This argument for stability, however, ignores the fact that the available free energy associated with a shear flow may be a potent source for the destabilization of some other class of fluctuations. The Kelvin-Helmholtz (KH) instability [1-3], for instance, is a well-known example of an instability that feeds on the ambient flow-energy. On the other hand, various discrepancies between theory and experiment regarding the stability limit of neutral fluids have been reported [4]. This is because rigorous treatment of the shear flow effects encounters a fatal difficulty arising from the non-Hermitian (non-self-adjoint) properties of the problem. The standard normal mode approach breaks down, and the theory may fail to provide correct predictions of evolution even if fluctuation remains in the linear regime.

Since the stability of an equilibrium has to be discussed for arbitrary initial conditions, it is important to find a general solution of the evolution equation governing linear dynamics. Fortunately, the linearized equation for a static (flow-less) equilibrium is described by a Hermitian (self-adjoint) operator when we determine the evolution equation in terms of the displacement vector [5-7]. Thus, as we normally do in conventional eigenvalue analysis, we may simply

author's e-mail: tatsuno@glue.umd.edu

This article is based on the invited talk at the 19th Annual Meeting of JSPF (Nov. 2002, Inuyama).

**Present address: Institute for Research in Electronics and Applied Physics, University of Maryland, College Park, Maryland 20742-3511, USA*

replace ∂_t by $-i\omega$ and see if the equilibrium may yield an exponentially unstable eigenvalue and corresponding eigenfunction. We may simply conclude that the equilibrium is unstable if we find at least one eigenvalue having a positive imaginary part of ω and if the corresponding eigenfunction has finite energy (non-divergent). The completeness of this spectral method is guaranteed only for Hermitian operator due to von Neumann's theorem [8,9]. However, the question on the stability problem is not answered yet when we do not find any unstable eigenvalue.

As we already mentioned, the problem is related to the completeness of the solutions. While it is well known that complete solutions to nonlinear equations are difficult to achieve, the difficulty of solving linear ones is less recognized. Even if we suppose that all eigenvalues are obtained, it's still very difficult to confirm if the obtained eigenfunctions sufficiently describe complete dynamics. Initially, the number of eigenvalues must be infinity for infinite-dimensional operators (eg., integral or differential operators), and worse, for the non-Hermitian operator, the eigenfunctions are not orthogonal to each other. In the case of finite-dimensional operators (eg., matrix operators), the Jordan matrix is the known example in which eigenvectors are not sufficient to describe complete dynamics. It is known that secular growth (algebraic in time) may lead to instability even if all eigenvalues show stability [10]. Recently such an algebraic instability has been pointed out to occur in the infinite-dimensional system due to the frequency overlapping between continuous spectra [11], and we may even observe an instability with fractional power in time [12]. We simply do not know what may happen in the infinite-dimensional non-Hermitian operators!

There are also many unresolved problems related to the physical understanding of the linear dynamics of shear flow plasmas. KH instability is one of the most famous instabilities in parallel shear flow systems, in which the background flow is stable unless its curvature changes sign in the domain. However, even the background shear flow having a linear profile (free from KH instability) can make the equilibrium more unstable when combined with an Alfvén wave [13]. While the stabilizing mechanisms of shear flow have been stressed, relatively little attention has been paid to its destabilizing effect. A shear flow may equally effectively destabilize a class of plasma modes even if the flow profile itself is stable.

In this paper, we describe both the mathematical and physical aspects of the recent developments in linear stability theories of shear flow plasmas. First, we introduce the linearized reduced MHD equation describing the incompressible motions of plasmas in Sec. **2**. We briefly review the energy principle and properties of spectra in static (flow-less) plasmas.

In Sec. **3**, we consider the surface-wave model (piece-wise linear shear flow profile) of two-dimensional vortex dynamics in neutral fluids. We first revise the Rayleigh's analysis of KH instability [14]. He did not directly manipulate the evolution equation of vorticity (Rayleigh equation), but his analysis gives us deep physical insight into the problem. Next, we briefly review the eigenvalue analysis of the Rayleigh equation and discuss how each term affects the system by comparison to Rayleigh's analysis. We also show the existence of degenerate frequencies (nilpotent) for a KH-stable wave number. Since the generator of the Rayleigh equation is non-Hermitian, the complete spectra may contain the infinite-dimension analogue of the Jordan block of a finite-dimension operator. Finally, we include the effect of gravity. We show that numerical integration shows localized secular behavior in the vorticity due to coupling of two continuous spectra [11]. This example shows that degenerate frequency spectra may give rise to the algebraic instability in non-Hermitian systems even if all eigenvalues (point or continuous spectra) are real.

In Sec. **4**, we show the stabilizing effect of shear flow due to its stretching effect by invoking Kelvin's method of shearing modes [15]. While this method has been previously called a 'nonmodal' approach in a wide range of literatures [16], it is shown as a particular case of a generalized 'modal' one [12,17,18]. We discuss the transient and secular behaviors of interchange fluctuations in Couette flow in an infinite interval. The combined effect of shear flow mixing and Alfvén wave propagation overcomes the instability driving force after sufficiently long periods, and damps all fluctuations of the magnetic flux with an inverse power of time. On the other hand, electrostatic perturbations can be destabilized for a sufficiently strong interchange drive. The time asymptotic behavior in each case is algebraic (non-exponential).

In Sec. **5**, we discuss the destabilizing effect of shear flow [13]. In contrast to its well-known stabilization of the low-frequency plasma motions, a shear flow may equally effectively destabilize a class of plasma modes. We focus on the latter quality of the flow by reviewing an incompressible ideal plasma having

Couette flow in a finite interval. In the presence of the flow shear, the growth rate of the perturbation increases due to the coupling of the Alfvén wave with a Rayleigh-Taylor type instability drive. Marginally stable modes in the flow-less equilibrium achieve their maximum growth rate when the maximum flow velocity becomes comparable to the Alfvén velocity. At larger shear flow velocities, however, the stabilizing "stretching" effect becomes dominant and the instability is quenched.

2. Reduced Magnetohydrodynamics and its Basic Properties

2.1 Formulation

In this article, we consider the ideal incompressible motion of plasmas in the fluid description.We restrict the geometry to a one-dimensional plane slab and highlight the fundamental structures from both mathematical and physical points of view.

In the Cartesian coordinates, we consider the equilibria in which the plasma current density is taken as $\boldsymbol{J}_0 = J_0 \boldsymbol{e}_z$, with $\boldsymbol{e}_z$ denoting the unit vector in the z direction, while a strong magnetic field is also applied in the z direction. We restrict the problem by assuming

$$\boldsymbol{V}_0 = (0, V_y(x), 0). \tag{1}$$

This situation is illustrated in Fig. 1.

Under the above conditions, we may assume that the perturbed fields come from two-dimensional incompressible motions and are written as

$$\boldsymbol{v}_1 = \nabla\phi \times \boldsymbol{e}_z, \quad \boldsymbol{b}_1 = \nabla\psi \times \boldsymbol{e}_z, \tag{2}$$

where ϕ and ψ denote the stream function and the flux function, respectively.

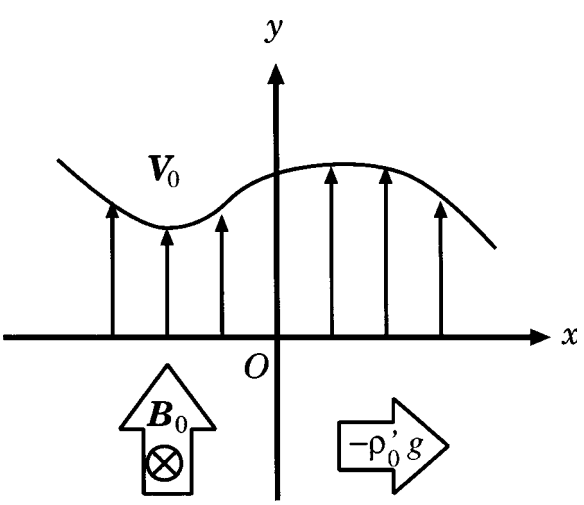

Flg. 1 Equilibrium configurations we consider in this paper.

In the linearized equation of motion, we neglect the variation of the density in the inertial term, but not in the gravitational force (Boussinesq approximation [1]). This derivation is almost parallel to that of Strauss [19] so that we do not describe it in detail here. By taking the curl of the equation of motion and projecting it on the z axis, we obtain the vorticity evolution equation;

$$\rho_0\left[\left(\partial_t + V_y\partial_y\right)\Delta\phi - V_y''\partial_y\phi\right] = \frac{1}{\mu_0}\boldsymbol{B}_0\cdot\nabla\Delta\psi + \left(\nabla J_0\times\boldsymbol{e}_z\right)\cdot\nabla\psi + g\partial_y\rho_1, \tag{3}$$

where $\Delta = \partial_x^2 + \partial_y^2$ denotes the two dimensional Laplacian operator. The continuity equation immediately reads

$$(\partial_t + V_y\partial_y)\rho_1 = -\rho_0'\partial_y\phi. \tag{4}$$

The induction equation is decurled to yield

$$(\partial_t + V_y\partial_y)\psi = \boldsymbol{B}_0\cdot\nabla\phi. \tag{5}$$

Equations (3)–(5) constitute a closed set of equations describing the linearized incompressible motion of the magnetized plasma. Actually, Eqs. (3)–(5) can be obtained by directly replacing $g = 2/R_0$ in the high β reduced MHD equations describing tokamak plasmas [20], where R_0 denotes the major radius of the toroidal device.

Let us examine the structure of the governing equations (3)–(5). In the flow-less case ($V_y = 0$), the left hand sides of Eqs. (3)–(5) only contain the time derivative. The first two terms on the right hand side of Eq. (3) and the right hand side of Eq. (5) correspond to the Alfvén wave. In homogeneous magnetic field, the ∇J_0 term disappears and we obtain the simple wave equation in which the phase velocity is given by the Alfvén velocity $\boldsymbol{v}_A = \boldsymbol{k}\cdot\boldsymbol{B}_0/\sqrt{\mu_0\rho_0}$. The last term of the right-hand side of Eq. (3) and right-hand side of Eq. (4) correspond to the effect of the gravity. When $\rho_0' > 0$, they yield a stable gravity wave propagating in the y direction, and when $\rho_0' < 0$, they yield interchange (Rayleigh-Taylor) instability. All these terms yield a Hermitian contribution in energy norm ($\int|\nabla\phi|^2\,dV$) as we show in Sec. **2.3**.

On the other hand, when we add finite flow, the left hand sides of Eqs. (3)–(5) become convective derivatives. If the flow is shear-less (V_y = const), these contribution yield simply the frequency shift (Doppler shift); however, once if it is sheared, the problem becomes non-Hermitian. The $V_y\partial_y$ terms in the convective

derivative are Hermitian in the *vorticity norm* $\int|\Delta\phi|^2 \mathrm{d}V$), but not in the energy norm. These terms may appear to add a simple multiplication operator if we assume a wave number k_y; however, the energy norm, which is suitable for other terms (including V_y'' term), makes them non-Hermitian [21]. Note that the left hand side of Eq. (3) yields the Rayleigh equation which describes Kelvin-Helmholtz instability when B_0 and ρ_0' are absent.

2.2 Hermiticity (selfadjointness) and energy principle for static equilibria

When the plasma equilibrium is static and uniform (V_y = 0, $\boldsymbol{B}_0$ = const, and ρ_0' = 0), the energy of the perturbed field in two-dimensions is conserved [see Eq. (2)];

$$\frac{\mathrm{d}}{\mathrm{d}t}\int\left[\frac{1}{2}(\rho v_1^2)+\frac{1}{2\mu_0}b_1^2\right]\mathrm{d}V=0\,. \tag{6}$$

When we introduce an inhomogeneity of the ambient magnetic field, however, the energy of the perturbed field contained in Eq. (6) is no longer a conserved quantity. We thus combine Eqs. (3)–(5) and obtain

$$\begin{aligned}&\rho_0\partial_t^2\Delta\phi\\&\quad=\frac{1}{\mu_0}\boldsymbol{B}_0\cdot\nabla\Delta\boldsymbol{B}_0\cdot\nabla\phi\\&\qquad+\left(\nabla J_0\times\boldsymbol{e}_z\right)\cdot\nabla\boldsymbol{B}_0\cdot\nabla\phi-\rho_0' g\,\partial_y^2\phi,\end{aligned} \tag{7}$$

where we still assume the static equilibrium (V_y = 0). Equation (7) is a second order evolution equation for vorticity $\Psi = -\Delta\phi$. When we consider a one-dimensional equilibrium (equilibrium quantities depend only on x), we may assume wave numbers (k_y and k_z) in the homogeneous directions (y and z directions). The second and the third terms in Eq. (7) then yield only multiplications on ϕ. Since the stream function reads $\phi = -\Delta^{-1}\Psi$, we find that the generator of Eq. (7) is Hermitian (selfadjoint) under the norm

$$\langle\Psi\,|\,\Psi\rangle:=-\int\bar{\Psi}\Delta^{-1}\Psi\,\mathrm{d}V=\int|\nabla\phi|^2\,\mathrm{d}V\,, \tag{8}$$

where the bar denotes the complex conjugate.

The mathematical grounds of Hermitian operators are fairly well developed in the context of quantum mechanics [22]. Namely, the spectra of a Hermitian operator consists of points and continua, their eigenvalues are real, and their eigenfunctions span the whole function space (von Neumann theorem; see Refs. [8,9]). Therefore, the general solution of an evolution equation governed by a Hermitian generator is obtained by means of the spectral resolution method. Since the eigenfunctions of Hermitian operators are independent and orthogonal with each other, we can draw information regarding the stability from the eigenvalue analysis. Thus we may replace ∂_t by $-\mathrm{i}\omega$ and the equilibrium is stable if and only if all ω corresponding to the eigenvalues of generator are real.

Moreover, we obtain a conserved quantity from the Hermiticity of the generator. Let us symbolically write Eq. (7) by

$$\rho_0\partial_t^2\Psi=F\,\Psi, \tag{9}$$

where the operator F is Hermitian and ρ_0 is a positive constant due to Boussinesq approximation. Then, the Hermiticity of F immediately yields

$$\frac{\mathrm{d}}{\mathrm{d}t}\left(\rho_0\langle\partial_t\Psi\,|\,\partial_t\Psi\rangle+\delta W\right)=0\,, \tag{10}$$

where

$$\delta W:=-\langle\Psi\,|F\,\Psi\rangle, \tag{11}$$

by taking the scalar products with $\partial_t\Psi$ on both sides of Eq. (9). The conserved quantity in Eq. (10) is also called energy, while it is different from the conventional one in Eq. (6). We also find from Eq. (9) the equality

$$\frac{\rho_0}{2}\frac{\mathrm{d}^2}{\mathrm{d}t^2}\langle\Psi\,|\,\Psi\rangle=\rho_0\langle\partial_t\Psi\,|\,\partial_t\Psi\rangle-\delta W\,. \tag{12}$$

Equations (10) and (12) lead to the energy principle [5-7], which states that the equilibrium is linearly stable if and only if

$$\delta W\geq 0\quad(\forall\Psi) \tag{13}$$

is satisfied. The sufficiency of the condition (13) immediately follows from the conservation law (10). The necessity is drawn from Eq. (12) [23], which indicates, if we find a normalized function whose bilinear form δW is negative, the existence of an eigenfunction of F whose eigenvalue $\lambda = -\omega^2$ is greater or equal to $-\delta W / \rho_0 > 0$.

2.3 Spectra of Alfvén waves in static equilibria

We consider the equilibrium magnetic field

$$\boldsymbol{B}=(0,\,B_y(x),\,B_z), \tag{14}$$

with B_z = const. From the homogeneity of the equilibrium quantities in the y and z directions, we may assume the wave numbers $\boldsymbol{k}$ = (0, k_y, k_z). Since the

generator is Hermitian as is seen in Sec. **2.2**, we may consider the eigenvalue λ of the generator when replacing ∂_t by $-i\omega$ ($\lambda = -\omega^2$). Then, Eq. (7) gives

$$\frac{\mathrm{d}}{\mathrm{d}x}\left[\left(\omega^2-\omega_{\mathrm{A}}^2\right)\frac{\mathrm{d}\phi}{\mathrm{d}x}\right]-k_y^2\left(\omega^2-\omega_{\mathrm{A}}^2\right)\phi+k_y^2\frac{\rho_0' g}{\rho_0}\phi=0\,, \tag{15}$$

where we have defined $F(x) = \boldsymbol{k}\cdot\boldsymbol{B}(x)$ and $\omega_{\mathrm{A}}(x) = F(x)/\sqrt{\mu_0\rho}$.

2.3.1 Alfvén continuum

Let us consider the case in which $\rho_0' = 0$. First we find a series of singular solutions. Equation (15) should not contain any singular solution except the Alfvén resonance ($\omega^2 - \omega_{\mathrm{A}}^2 = 0$) [24]. Suppose that $\omega^2 - \omega_{\mathrm{A}}^2(x)$ has the zero of the order h ($\in$N) at $x = x_{\mathrm{s}}$, i.e.,

$$\omega^2 - \omega_{\mathrm{A}}^2(x) = c(x)\,(x - x_{\mathrm{s}})^h, \tag{16}$$

where $c(x)$ is an analytic function with finite value at $x = x_{\mathrm{s}}$. For investigating the behavior of the solution in the vicinity of the singular point x_{s}, we take the leading order of the Taylor expansion (16) and substitute it into Eq. (15), which yields

$$\frac{\mathrm{d}^2\phi}{\mathrm{d}x^2}+\frac{h}{x-x_s}\frac{\mathrm{d}\phi}{\mathrm{d}x}+k_y^2\phi=0\,. \tag{17}$$

We thus find that the point $x = x_{\mathrm{s}}$ is a regular singular point of the ODE (15) for any $h \in$ N. By means of the Frobenius expansion [25], we obtain a logarithmic singularity in the solution since two solutions of the indicial equation have an integral difference for any h [26];

$$\phi(x) = a_1 g_1(x) + a_2[g_1(x)\log|x - x_{\mathrm{s}}| + g_2(x)], \tag{18}$$

where $g_1(x)$ and $g_2(x)$ are analytic functions with $g_1(x_{\mathrm{s}}) \neq 0$. When we apply the energy norm (8) to the solution (18), which now reads

$$\langle\phi\,|\,\phi\rangle = -\int \bar{\phi}\,\Delta\phi\;\mathrm{d}V\,, \tag{19}$$

we then find that Eq. (18) actually gives a non-square-integrable solution corresponding to the continuous spectrum [27]. We can show that Eq. (15) with $\rho_0' = 0$ has no other spectrum than the Alfvén continuum [21].

2.3.2 Interchange mode

When $\rho_0' \neq 0$ in Eq. (15), the singularity is no longer regular if the zero of Eq. (16) is not simple ($h > 1$). In this case, we do not have a general explicit representation of the singular solution. Moreover, the last term in Eq. (15) admits the point spectra.

Let us briefly represent the case ρ_0', B_y = const in order to highlight the essential properties of the point spectra. In this case, Eq. (15) yields

$$\frac{\mathrm{d}^2\phi}{\mathrm{d}x^2}-k_y^2\left(1+\frac{G}{\omega^2-k_{\|}^2}\right)\phi=0\,, \tag{20}$$

where $k_{||} = \boldsymbol{k}\cdot\boldsymbol{B}/|\boldsymbol{B}|$ (= const) is the wave number parallel to the ambient magnetic field. For the eigenfunctions to satisfy the boundary conditions, we need

$$k_{\|}^2 - G < \omega^2. \tag{21}$$

Since $k_{||}^2 > 0$, the Alfvén wave acts to stabilize interchange modes. If Eq. (21) is satisfied, we obtain even and odd eigenmodes;

$$\phi = \begin{cases} \cos(n\pi x/2) & \text{for } n\text{: odd} \\ \sin(n\pi x/2) & \text{for } n\text{: even} \end{cases}, \tag{22}$$

respectively. The eigenmodes contain $n - 1$ nodes (zeros in ϕ). The dispersion relation is

$$\omega^2 = k_{\|}^2 - \frac{k_y^2 G}{k_y^2 + n^2\pi^2/4}\,, \tag{23}$$

showing that ω^2 decreases monotonically as $|k_y|$ increases.

The upper bound of ω^2 is $k_{||}^2$, which is the accumulation point of ω_n^2 as $n \to \infty$; i.e.,

$$k_{\|}^2 - G < \omega^2 < k_{\|}^2\,. \tag{24}$$

The distribution of the eigenvalues is illustrated in Fig. 2, which represents a typical spectral structure of the discrete part of the shear Alfvén branch [29]. If $k_{||}^2$, is larger than the drive G, there is no instability even if $G > 0$. The instability condition is given by

$$G > k_{\|}^2\left(1+\frac{\pi^2}{4k_y^2}\right). \tag{25}$$

In more general cases, the following facts are known. Due to Sturm's oscillation theorem [25], we will have an unstable eigenvalue $\omega^2 < 0$ which satisfies the boundary condition on both sides if the solution for $\omega^2 =$

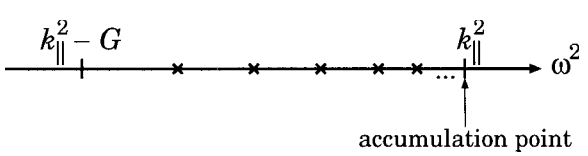

Fig. 2 Distribution of eigenvalues in ω^2 space.

0 satisfying the boundary condition only on one edge has any node in the domain [28]. Furthermore, the number of these point spectra are infinite, which accumulate on the edge of the continuum $\omega^2 = \inf \omega_A^2$ [29]. When the smallest eigenvalue is positive and the mode has no resonant surface inside the plasma, the eigenfunction shows a global stable oscillation, which is similar to the global Alfvén eigenmode [30].

3. Surface Wave Model of Rayleigh Equation

In this section, we focus on the Rayleigh equation

$$\partial_t \Delta\phi + V_y \partial_y \Delta\phi - V_y'' \partial_y \phi = 0, \tag{26}$$

under the velocity profile shown in Fig. 3. We may derive Eq. (26) from Eq. (3) by neglecting magnetic field ($\boldsymbol{B}_0 = \boldsymbol{0}$) and gravity ($\boldsymbol{g} = \boldsymbol{0}$). It is noted that the assumption of a strong B_{0z} in deriving Eq. (3) does not create a problem because it directly takes into account the curl of the original fluid equation under the incompressibility condition.

3.1 Rayleigh's analysis

Rayleigh had first introduced the piece-wise linear shear flow profile for the analysis of KH instability [14]. His discussion was directly related to the surface displacement which separates the distinct vorticity regions. By following his analysis, we will discuss the physical aspects of this issue in this subsection.

Suppose a stationary shear flow profile as illustrated in Fig. 3. The profile of the velocity field consists of two constant regions ($x < -a$ and $a < x$) and a single linear shear ($-a < x < a$) region. Thus, the vorticity field is constant $\sigma = U/a$ in $-a < x < a$ and zero elsewhere.

Suppose that we deform the boundary surface on $x = a$ by an infinitesimally small amount

$$\xi_1(y,t) = H_1 e^{i(ky-\omega t)}, \tag{27}$$

where H_1 denotes the complex amplitude. Since the vorticity is discontinuous around $x = a$, deformation of the surface induces perturbed velocity into the system.

By a theorem due to Helmholtz [14], the infinitesimally small area element dA with the z-directed vorticity σ induces the transverse velocity

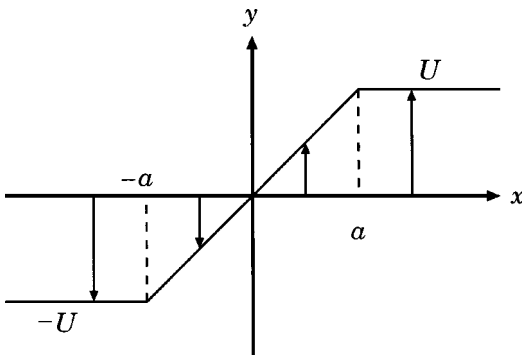

Fig. 3 Rayleigh's piece-wise linear shear flow profile.

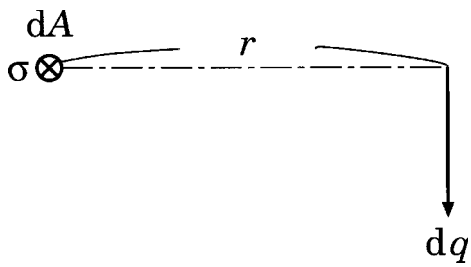

Fig. 4 Helmholtz' principle, which gives the integral kernel of the operator $(\nabla\times)^{-1}$.

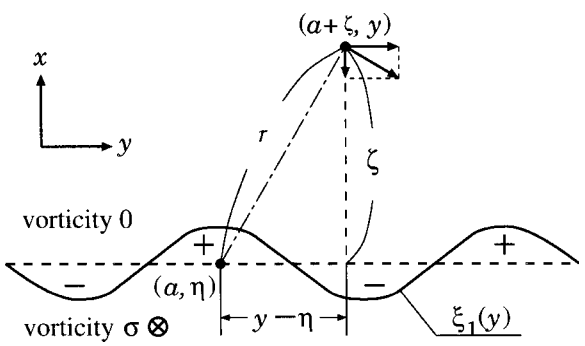

Fig. 5 Surface displacement at (a,η) produces the velocity field at $(a + \zeta, y)$.

$$dq = \frac{\sigma dA}{2\pi r}, \tag{28}$$

where r denotes the distance from the element (see Fig. 4). This corresponds to the integral kernel of the operator $(\nabla\times)^{-1}$ [1]. In the case of surface deformation shown by Eq. (27), we obtain the velocity at $(a + \zeta, y)$ induced by the surface element $\xi_1\, d\eta$ at (a,η) as

[1] In three dimensions, the operator $(\nabla\times)^{-1}$ is described by $\boldsymbol{v}(\boldsymbol{r}) = \frac{1}{4\pi}\int \Omega(\boldsymbol{r}') \times \frac{\boldsymbol{r}-\boldsymbol{r}'}{|\boldsymbol{r}-\boldsymbol{r}'|^3} d\boldsymbol{r}'$ in the infinite domain. Integrating it with respect to z from $-\infty$ to ∞, we obtain Eq. (28).

$$\mathrm{d}q = \frac{\sigma \xi_1 \,\mathrm{d}\eta}{2\pi r}, \tag{29}$$

where $r^2 = (y-\eta)^2 + b^2$. Taking the x component of the velocity dq yields

$$\mathrm{d}v_{1x} = \frac{\eta - y}{r}\,\mathrm{d}q = \frac{H_1\,\sigma}{2\pi}\,\frac{(\eta-y)\,\mathrm{e}^{\omega t}}{r^2}\,\mathrm{e}^{-\mathrm{i}\omega t}\mathrm{d}\eta. \tag{30}$$

Integrating Eq. (30) with respect to η yields the velocity field at $(a+\zeta, y)$ induced by the whole surface displacement on $x = a$

$$v_{1x} = \frac{H_1\,\sigma}{2\pi}\,\mathrm{e}^{-\mathrm{i}\omega t}\int \frac{(\eta-y)\,\mathrm{e}^{\mathrm{i}k\eta}}{r^2}\,\mathrm{d}\eta. \tag{31}$$

$$= \frac{\mathrm{i}H_1\,\sigma}{2}\,\mathrm{e}^{-k|\zeta|}\,\mathrm{e}^{\mathrm{i}(ky-\omega t)}, \tag{32}$$

where we have used the formula

$$\int_{-\infty}^{\infty} \frac{x\sin(\alpha x)}{\beta^2 + x^2}\,\mathrm{d}x = \pi \mathrm{e}^{-\alpha\beta}. \tag{33}$$

On the other hand, the evolution equation for the perturbed surface is governed by

$$\partial_t \xi_{1,2} = v_{1x} - V_y \partial_y \xi_{1,2}, \tag{34}$$

where

$$\xi_2(y,t) = H_2 \mathrm{e}^{\mathrm{i}(ky-\omega t)} \tag{35}$$

denotes the surface displacement on $x = -a$. The first term on the right hand side in Eq. (34) implies the transfer of the surface due to perturbed velocity, and the second one, the stretching effect of the ambient flow. The y component of the perturbed velocity is omitted since it gives a higher order contribution with the combination of $\partial_y \xi_{1,2}$. We thus estimate the perturbed velocities on $x = \pm a$ by putting $\zeta = 0$ and $\zeta = \pm 2a$ in Eq. (32), which yields

$$v_{1x}(a,y,t) = \frac{\mathrm{i}\sigma}{2}\,\mathrm{e}^{\mathrm{i}(ky-\omega t)}\left(H_1 - H_2\,\mathrm{e}^{-2ka}\right), \tag{36}$$

$$v_{1x}(-a,y,t) = \frac{\mathrm{i}\sigma}{2}\,\mathrm{e}^{\mathrm{i}(ky-\omega t)}\left(H_1\,\mathrm{e}^{-2ka} - H_2\right). \tag{37}$$

Substituting Eqs. (36) and (37) into Eq. (34), we obtain

$$\left(1 - 2ka + 2\,\frac{\omega}{\sigma}\right)H_1 - \mathrm{e}^{-2ka}\,H_2 = 0, \tag{38}$$

$$\mathrm{e}^{-2ka}\,H_1 - \left(1 - 2ka - 2\,\frac{\omega}{\sigma}\right)H_2 = 0. \tag{39}$$

The consistency condition finally yields the dispersion relation

$$\omega^2 = \frac{\sigma^2}{4}\left[\left(2ka-1\right)^2 - \mathrm{e}^{-4ka}\right]. \tag{40}$$

The unstable branch of Eq. (40) is

$$\omega = \mathrm{i}\,\frac{\sigma}{2}\sqrt{\mathrm{e}^{-4ka} - \left(2ka-1\right)^2}, \tag{41}$$

when $|(2ka-1)\mathrm{e}^{2ka}| < 1$. The corresponding eigenstate has the relative amplitude of the surface displacement

$$\frac{H_2}{H_1} = (1-2ka)\,\mathrm{e}^{2ka} + \mathrm{i}\sqrt{1-(1-2ka)^2\,\mathrm{e}^{4ka}} = \mathrm{e}^{\mathrm{i}(\pi-\theta)}, \tag{42}$$

where

$$\mathrm{e}^{-\mathrm{i}\theta} := (2ka-1)\,\mathrm{e}^{2ka} - \mathrm{i}\sqrt{1-(2ka-1)^2\,\mathrm{e}^{4ka}}. \tag{43}$$

For the sake of simplicity, suppose $ka = 1/2$ ($\theta = \pi/2$). In this case, $v_{1x}(a,y,t)$ induced by the surface ξ_1 itself exactly cancels the convective derivative term. Therefore, the surface displacement is locked in the laboratory frame due to the velocity field induced by itself (ξ_1), and is amplified due to that induced by the other (ξ_2).

The schematic view of the unstable eigenstate Eq. (42) is illustrated in Fig. 6. The perturbed velocity induced by the deformation H_1 at the surface $x = a$ is represented by the straight arrows. Since we assumed the $\mathrm{e}^{\mathrm{i}ky}$ dependence on ξ_1 and ξ_2, Eq. (42) implies that the phase ξ_2 advances in y direction with respect to ξ_1 by an amount $\pi - \theta$. Thus, the velocity field induced by the perturbed vorticity field on $x = a$ indicates the direction of the amplification of the surface displacement on $x = -a$, and vice versa. The perturbation grows exponentially due to the mutual interaction of two phase-shifted surface displacements.

The contour plot of the stream function $\phi = K\Psi$ corresponding to the unstable eigenmode is shown in Fig. 7 ($k = 0.5$ and $a = 1$). In this figure, we take the x-

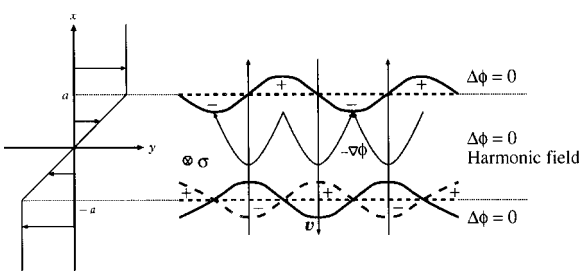

Fig. 6 Schematic view for the unstable eigenfunction (42) or (62) of Kelvin-Helmholtz instability.

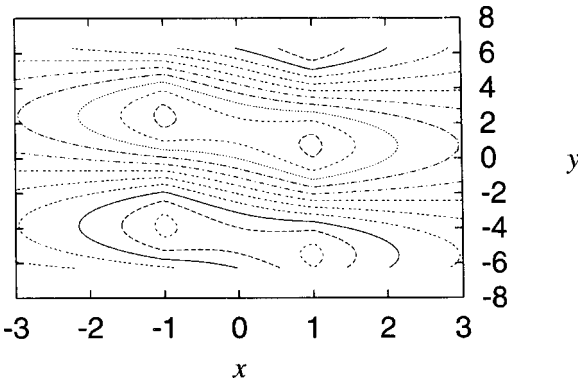

Fig. 7 Contour plot of the real part of stream function. The figure is plotted for $k = 0.5$ and $a = 1$.

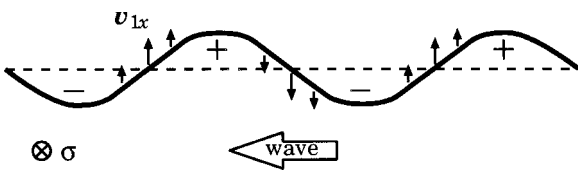

Fig. 8 Surface wave due to vorticity variation.

axis in the horizontal direction. We observe that $V_y' v_x v_y < 0$ is satisfied throughout in the finite flow shear region ($-1 < x < 1$) [see Eq. (143) in Sec. **5.2**]. The damped mode has an opposite phase difference between surface waves, which yields the opposite inclination of the flow pattern. While the ambient shear flow is in the positive y-direction in $x > 0$ and toward the negative in $x < 0$, the mode structure is inclined in the opposite direction to it. This may be attributed to the surface wave which we will describe in the following section.

In order to see the surface wave explicitly, it is helpful to consider the case of a single surface of vorticity separation. The surface displacement will produce the velocity field v_{1x} with $\pi/2$ out-of-phase [see Eq. (36)]. Due to this effect, the surface displacement can propagate as a wave with respect to the rest frame of the fluid (see Fig. 8). The dispersion relation of the surface wave appears as

$$\omega = -\frac{\sigma}{2}, \tag{44}$$

whose phase velocity is

$$v_{\mathrm{ph}} = -\frac{\sigma}{2k}. \tag{45}$$

Thus, the vorticity variation becomes a source of the wave which corresponds to the V_y'' term in Eq. (26). It is, therefore, deduced that the surface wave propagates in the opposite direction to the ambient flow, which supports the mode for escaping from the stretching effect.

When wave number k is small, the phase velocity v_{ph} of the surface wave is so large that it has a high capability for the transfer of the vorticity, while the velocity of the ambient flow is fixed (U). As k becomes large, the phase velocity v_{ph} becomes small, and the maximum growth rate is achieved around $|v_{\mathrm{ph}}| \simeq |V_y|$. Namely, the mode becomes the most unstable when the surface wave tends to stop due to the effect of background flow. If the wave number k is too large, the phase velocity v_{ph} becomes so small that it cannot compete with the background flow. In other words, the x component of the velocity created from the ambient flow $V_y \partial_y \xi_{1,2}$ is too large in Eq. (34), and v_{1x} of itself cannot afford to lock the surface. Thus, the instability will be suppressed.

3.2 Eigenvalue analysis

In this section, we define a generalized Rayleigh equation

$$\mathrm{i}\partial_t \Psi = L\Psi \tag{46}$$

$$L := kV_y(x) + kW(x)K \tag{47}$$

in the infinite domain ($x \in \mathrm{R}$), where the Green operator K is represented by a convolution integral

$$(Kf)(x) = \int_{-\infty}^{+\infty} \frac{\mathrm{e}^{-k|x-\xi|}}{2k} f(\xi)\,\mathrm{d}\xi\,. \tag{48}$$

In the following, we denote the Green function by $K(x,\xi)$;

$$K(x,\xi) = \frac{\mathrm{e}^{-k|x-\xi|}}{2k}. \tag{49}$$

In Eq. (47), we take $V_y(x)$ and $W(x)$ to be independent arbitrary functions. The case in which $W(x) = V_y''(x)$ recovers the physically relevant equation (26).

Firstly, let us assume $W(x) = 0$ in Eq. (47) and consider

$$\mathrm{i}\partial_t \Psi = kV_y(x)\Psi \tag{50}$$

with a continuous real function $V_y(x)$. The formal eigenvalue λ and the corresponding eigenfunction φ of the generator of Eq. (50) are given by

$$\lambda = kV_y(\mu), \quad \varphi = \delta(x-\mu), \tag{51}$$

where μ is an arbitrary real number. The solution of Eq. (50) with initial condition $\Psi(x,0)$, thus, yields

$$\Psi(x,t) = \mathrm{e}^{-\mathrm{i}tkV_y(x)}\Psi(x,0). \tag{52}$$

Second, we assume

$$V_y(x) = 0, \tag{53}$$

$$W(x) = -\sigma\delta(x-a), \tag{54}$$

then the operator reads

$$L_1 = -\frac{\sigma}{2}\delta(x-a)\int_{-\infty}^{\infty} \mathrm{e}^{-k|x-\xi|}\,\mathrm{d}\xi\,. \tag{55}$$

The eigenvalue and the corresponding eigenfunction of L_1 are, respectively,

$$\lambda = -\frac{\sigma}{2}, \quad \varphi(x) = \delta(x-a)\,. \tag{56}$$

Eigenmode (56) corresponds to the surface wave (44). When we include another surface of different vorticity regions and assume

$$W(x) = -\sigma\,[\delta(x-a) - \delta(x+a)], \tag{57}$$

the corresponding eigenvalues and eigenfunctions of the resulting operator L_2 are

$$\lambda = \pm\frac{\sigma}{2}\sqrt{1-\mathrm{e}^{-4ka}}\,,$$
$$\varphi(x) = \delta(x-a) - \left(1 \pm \sqrt{1-\mathrm{e}^{-4ka}}\right)\mathrm{e}^{2ka}\,\delta(x+a)\,. \tag{58}$$

Then, we may formally write the operator L_2 in the matrix form by means of the basis vectors $\delta(x-a)$ and $\delta(x+a)$,

$$L_2 = \frac{\sigma}{2}\begin{pmatrix} -1 & -\mathrm{e}^{-2ka} \\ \mathrm{e}^{-2ka} & 1 \end{pmatrix}. \tag{59}$$

These oscillations represent the coupled surface modes which are excited on both surfaces $x = \pm a$. Note that these modes are stable for positive k in the absence of continuous spectra. Since the governing equation is the same as in the case of diocotron instabilities in non-neutral plasmas [31,32], these oscillations are called 'diocotron oscillations.'

The flow profile $V_y(x)$ discussed in Sec. **3.1** is accompanied by the $W(x)$ of Eq. (57). Let us consider the consistent profile given in Fig. 3 [$V_y''(x) = W(x)$] and denote the resulting operator by L_3. Then, by focusing on the subspace spanned by the two surface waves $\delta(x-a)$ and $\delta(x+a)$, we may obtain the following matrix form for the operator L_3;

$$L_3 = \begin{pmatrix} kU & 0 \\ 0 & -kU \end{pmatrix} + L_2\,. \tag{60}$$

Two eigenvalues of the 2×2 matrix L_3 denote the KH mode [1], whose dispersion relation reads

$$\lambda^2 = \frac{\sigma^2}{4}\left[(1-2ka)^2 - \mathrm{e}^{-4ka}\right]. \tag{61}$$

When $|(2ka-1)\mathrm{e}^{-2ka}| < 1$, the unstable branch of Eq. (61) yields

$$\lambda_- = \mathrm{i}\,\frac{U}{2a}\sqrt{\mathrm{e}^{-4ka} - (2ka-1)^2}\,,$$
$$\varphi_- = \delta(x-a) + \mathrm{e}^{-\mathrm{i}\theta}\,\delta(x+a)\,. \tag{62}$$

Because of the $\mathrm{e}^{\mathrm{i}ky}$ dependence of the vorticity, the eigensolution (62) states that the phase of the surface wave on $x = a$ advances in y direction to that on $x = -a$ by an angle θ ($0 < \theta < \pi$) [see Eqs. (41)–(43)].

This expression exactly coincides with the situation illustrated in Fig. 6. According to the surface wave perturbation of the form of Eq. (62), we plot the coefficient of the δ-function by the solid curve on $x = a$ in the right figure. Since the phase of the surface wave on $x = a$ advances in y direction to that on $x = -a$ by the angle θ, we may plot the amplitude of the surface wave on $x = -a$ by the dashed curve. Since the ambient vorticity is positive in $-a < x < a$ and zero elsewhere, we can directly regard the perturbed amplitude on $x = a$ as an illustration of the surface displacement which separates the two different vorticity region. However, the surface displacement on $x = -a$ is inverted from the perturbed amplitude of the vorticity because of the ambient vorticity field (positive in upward and zero in lower), which yields the illustration of the surface displacement by the solid curve.

Let us close this section by considering the effect

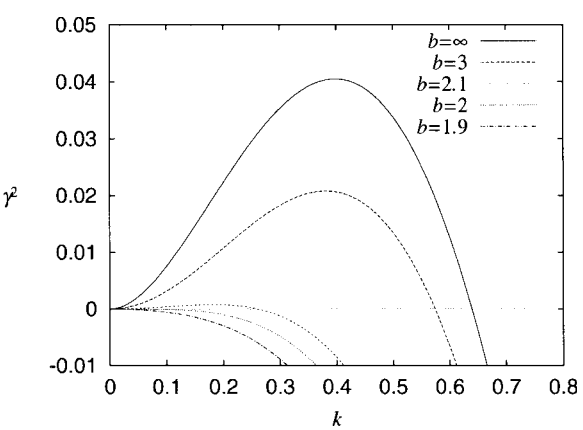

Fig. 9 Square of the growth rate when rigid wall is put along $x = \pm b$. The values of b are normalized by a.

of the finite domain size by putting a rigid boundary at $x = \pm b$ ($b > a$). The boundary condition for finite k_y yields $\phi = 0$ on $x = \pm b$. The dispersion relation then reads

$$\frac{\omega^2}{\sigma^2} = k^2 a^2 - \frac{2ka\left[(1+X)+(1-X)\,\mathrm{e}^{-4ka}\right] - 1 + \mathrm{e}^{-4ka}}{(1+X)^2 - (1-X)^2\,\mathrm{e}^{-4ka}}, \tag{63}$$

where

$$1 < X = \frac{1+\mathrm{e}^{-2k(b-a)}}{1-\mathrm{e}^{-2k(b-a)}} < \infty. \tag{64}$$

By assuming $\varepsilon := ka \ll 1$ with a and $b - a$ kept finite, we can put $1/X \simeq k(b-a) \ll 1$ and Eq. (63) is approximated to $O(\varepsilon^2)$ by

$$\frac{\omega^2}{\sigma^2} \simeq \frac{a^2}{b}\, k^2 (2a - b). \tag{65}$$

If b/a becomes smaller than 2, the KH mode may be stabilized (ω^2 becomes positive in $k \ll 1$). Dispersion relation (63) is numerically plotted in Fig. 9, which clearly shows that the KH mode is stabilized for all wave numbers when $b/a < 2$.

3.3 Nilpotent and resonance

We have studied the eigenmodes consisting of the Rayleigh equation in the previous section. The frequency of the surface wave is negative in the fluid frame; therefore, the eigenvalues of Eqs. (51) and (56) [or Eq. (61)] may overlap when $|(2ka-1)\mathrm{e}^{-2ka}| > 1$ is satisfied. Frequency overlapping between modes in non-Hermitian systems may cause algebraic instabilities even if all eigenvalues are real. In this section, we show the effect coming from such resonance or frequency overlapping.

For simplicity, we consider the single surface of vortical discontinuity (54) in Sec. **3.3.1**, and next consider the double-surface system corresponding to Eq. (57) in Sec. **3.3.2**. Here, the velocity field $V_y(x)$ is taken as consistent to $W(x)$.

3.3.1 Single surface system

Let us first consider the following case

$$L_4 = kV_y(x) - \frac{\sigma}{2}\,\delta(x-a)\int_{-\infty}^{\infty} \mathrm{e}^{-k|x-\xi|}\,\mathrm{d}\xi, \tag{66}$$

$$V_y(x) = \begin{cases} \sigma x & (x < a) \\ U & (a \le x) \end{cases}, \tag{67}$$

where $\sigma = U/a$. By assuming $\varphi \propto \mathrm{e}^{-\mathrm{i}\lambda t}$, we may obtain the following eigenvalue problem.

$$\lambda\varphi(x) = kV_y(x)\varphi(x) - \frac{\sigma}{2}\,\delta(x-a)\int_{-\infty}^{\infty} \mathrm{e}^{-k|x-\xi|}\,\varphi(\xi)\,\mathrm{d}\xi. \tag{68}$$

For this eigenvalue problem, we have the following sets of eigenvalues and the corresponding eigenfunctions:

1. For $\lambda_0 = kU$; the corresponding eigenfunctions are arbitrary continuous functions $\varphi_0(x)$ which satisfy

$$\int_a^{\infty} \mathrm{e}^{k(a-\xi)}\varphi_0(\xi)\,\mathrm{d}\xi = 0, \quad \text{and} \quad \varphi_0(x) = 0\ (x \le a). \tag{69}$$

2. For $\lambda_1 = kU - \sigma/2$; the corresponding eigenfunction is

$$\varphi_1(x) = \delta(x-a). \tag{70}$$

3. For $\lambda_\mu = kU\mu/a$ ($\mu < a$ and $\mu \neq a - 1/2k$); the corresponding eigenfunctions are

$$\varphi_\mu(x) = \delta(x-\mu) + \frac{\mathrm{e}^{-k(a-\mu)}}{2k(a-\mu)-1}\,\delta(x-a). \tag{71}$$

However, these eigenvalues are not complete and we have another eigenfunction in a wider sense (nilpotent). That is $\varphi_2(x) = \delta(x-\mu_0)$ where $\mu_0 := a - 1/2k$. We can easily see that

$$(\lambda_1 - L_4)\varphi_2(x) = \frac{U}{2a}\,\mathrm{e}^{-k(a-\mu_0)}\varphi_1(x). \tag{72}$$

Of course $(\lambda_1 - L_3)^2\varphi_2(x) = 0$ also holds. These relations are quite similar to the nilpotent in the finite dimension operator. Thus we may write the operator L_4 in the following matrix form including the case $\mu = \mu_0$:

$$L_3 = \begin{pmatrix} kU - \dfrac{\sigma}{2} & -\dfrac{\sigma}{2}\,\mathrm{e}^{-k(a-\mu)} \\ 0 & k\sigma\mu \end{pmatrix}, \tag{73}$$

where a Jordan block is obtained for $kU - \sigma/2 = \mathrm{k}\sigma\mu$ ($\mu = \mu_0$).

Let us evaluate the time evolution of the perturbation when we have taken this $\varphi_2(x)$ as an initial condition. As we can see from Eq. (72), we will have $\varphi_1(x)$ component by applying the generator L_4 to the initial condition $\varphi_2(x)$. Here we may consider the evolution to be closed in the subspace spanned by $\varphi_1(x)$ and $\varphi_2(x)$. Then, it is natural to expand Ψ as

$$\Psi(x,t) = \sum_{i=1}^{2} \alpha_i(t)\varphi_i(x). \tag{74}$$

Substituting Eq. (74) into the original equation (46), we obtain

$$\mathrm{i}\,\partial_t(\alpha_1\varphi_1+\alpha_2\varphi_2)=\left(\lambda_1\alpha_1-\frac{U}{2\alpha\sqrt{\mathrm{e}}}\,\alpha_2\right)\varphi_1+\lambda_1\varphi_2\,. \tag{75}$$

When we decompose Eq. (75) into φ_1 and φ_2, we obtain the time evolution of α_1

$$\alpha_1(t)=\left[\mathrm{i}\frac{\sigma}{2\sqrt{\mathrm{e}}}\,\alpha_2(0)t+\alpha_1(0)\right]\mathrm{e}^{-\mathrm{i}\lambda_1 t}\,, \tag{76}$$

where $\alpha_{1,2}(0)$ denote initial values. We find that for $\alpha_2(0) \neq 0$, we have a secular growth due to the resonance of the diocotron mode with one of the singular eigenfunctions in the continuous spectrum.

3.3.2 Rayleigh's system

Let us consider the case shown in Fig. 3. The generator is written as

$$L_5=kV_y(x) -\frac{\sigma}{2}\left[\delta(x-a)-\delta(x+a)\right]\int_{-\infty}^{\infty}\mathrm{e}^{-k|x-\xi|}\,\mathrm{d}\xi\,, \tag{77}$$

where the velocity field is defined by

$$V_y(x)=\begin{cases}-U & (x\le -a)\\ \sigma x & (-a<x<a)\\ U & (a\le x)\end{cases}. \tag{78}$$

Note that we consider the case $|(2ka-1)\mathrm{e}^{2ka}|>1$, where KH mode is exponentially stable.

If we set the basis vectors as $\varphi_1(x)=\delta(x-a)$, $\varphi_\mu(x)=\delta(x-\mu)$, and $\varphi_3(x)=\delta(x+a)$, we can obtain the following matrix representation for the operator L_5;

$$L_5=\frac{\sigma}{2}\begin{pmatrix}2ka-1 & -\mathrm{e}^{-k(a-\mu)} & -\mathrm{e}^{-2ka}\\ 0 & 2k\mu & 0\\ \mathrm{e}^{-2ka} & \mathrm{e}^{-k(a+\mu)} & -(2ka-1)\end{pmatrix}. \tag{79}$$

When we expand the perturbed vortex field

$$\Psi(x,t)=\sum_{i=1}^{3}\alpha_i(t)\varphi_i(x)\,, \tag{80}$$

regarding φ_2 as one of the φ_μ corresponding to a certain μ, and substitute Eq. (80) into the Rayleigh equation, we obtain

$$\mathrm{i}\frac{\mathrm{d}\alpha_1}{\mathrm{d}t}=\frac{\sigma}{2}\left[(2ka-1)\alpha_1-\mathrm{e}^{-k(a-\mu)}\alpha_2-\mathrm{e}^{-2ka}\alpha_3\right], \tag{81}$$

$$\mathrm{i}\frac{\mathrm{d}\alpha_2}{\mathrm{d}t}=k\sigma\mu\alpha_2\,, \tag{82}$$

$$\mathrm{i}\frac{\mathrm{d}\alpha_3}{\mathrm{d}t}=\frac{\sigma}{2}\left[\mathrm{e}^{-2ka}\alpha_1+\mathrm{e}^{-k(a+\mu)}\alpha_2-(2ka-1)\alpha_3\right]. \tag{83}$$

We find in the eigenvalues the coupling between two diocotron oscillations

$$\lambda_1^{\dagger}=\frac{\sigma}{2}\,\mathrm{e}^{-2ka}\sinh\psi\,, \tag{84}$$

$$\lambda_3^{\dagger}=-\frac{\sigma}{2}\,\mathrm{e}^{-2ka}\sinh\psi\,, \tag{85}$$

and the corresponding eigenfunctions are

$$\varphi_1^{\dagger}(x)=\delta(x-a)+\mathrm{e}^{-\psi}\delta(x+a), \tag{86}$$

$$\varphi_3^{\dagger}(x)=\mathrm{e}^{-\psi}\delta(x-a)+(x+a), \tag{87}$$

where $\cosh\psi=(2ka-1)\mathrm{e}^{2ka}$. By introducing new coefficients

$$\begin{pmatrix}\beta_1\\ \beta_3\end{pmatrix}=\frac{2}{\sinh\psi}\begin{pmatrix}\mathrm{e}^{\psi} & -1\\ -1 & \mathrm{e}^{\psi}\end{pmatrix}\begin{pmatrix}\alpha_1\\ \alpha_3\end{pmatrix}, \tag{88}$$

we may diagonalize the diocotron modes, which yields

$$\mathrm{i}\frac{\mathrm{d}\beta_1}{\mathrm{d}t}=\lambda_1^{\dagger}\beta_1 -\frac{\sigma}{\sinh\psi}\left[\mathrm{e}^{-k(a-\mu)}\mathrm{e}^{\psi}+\mathrm{e}^{-k(a+\mu)}\right]\alpha_2\,, \tag{89}$$

$$\mathrm{i}\frac{\mathrm{d}\alpha_2}{\mathrm{d}t}=k\sigma\mu\,\alpha_2\,, \tag{90}$$

$$\mathrm{i}\frac{\mathrm{d}\beta_3}{\mathrm{d}t}=\lambda_3^{\dagger}\beta_3 +\frac{\sigma}{\sinh\psi}\left[\mathrm{e}^{-k(a-\mu)}+\mathrm{e}^{-k(a+\mu)}\mathrm{e}^{\psi}\right]\alpha_2\,. \tag{91}$$

The solution of Eq. (90) is given by

$$\alpha_2(t)=\alpha_2(0)\,\mathrm{e}^{-\mathrm{i}k\sigma\mu t}. \tag{92}$$

When we assume

$$k\sigma\mu=\lambda_1^{\dagger}\ \text{ or }\ \lambda_3^{\dagger}, \tag{93}$$

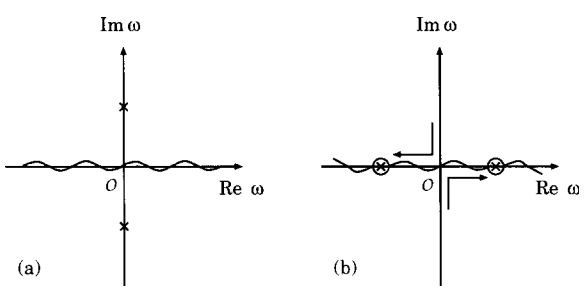

Fig. 10 Schematic view of the spectra for the KH (a) unstable and (b) stable systems. The crosses and wavy lines denote point and continuous spectra, respectively. Point spectra are embedded in the continua for KH stable case. Open circles denote the vacancy of continua (corresponding to nilpotent).

then we might have secularity due to the resonance with the simple oscillator $\varphi_2^\dagger$. On the other hand, we *do not* have it when the eigenvalues $\lambda_3^\dagger$ are complex or pure imaginary, namely when the system is unstable in a KH sense (see Fig. 10).

3.4 Coupling with gravity wave and secularity

In this section, we include the density gradient into the Rayleigh equation, and show that the coupling to the gravity wave will introduce a localized secular behavior. The continuity equation (4) couples with the equation of motion (3).

We consider the following stationary state:

$$V_y(x) = \begin{cases} -U \\ Ux/a \\ U \end{cases}, \qquad \rho_0(x) = \begin{cases} \rho^0 \mathrm{e}^{-\alpha a/g} & (x < -a) \\ \rho^0 \mathrm{e}^{-\alpha x/g} & (-a < x < a) \\ \rho^0 \mathrm{e}^{\alpha a/g} & (a < x) \end{cases}, \tag{94}$$

where U, a, and ρ^0 are constants. Let us normalize the variable by a for length and a/U for time. By introducing a new variable $\chi := \rho_1/\rho_0'$ and normalizing it by /a, we obtain

$$\mathrm{i}\partial_t \Psi = kV_y\Psi + kV_y''\phi + kv_g^2\chi \tag{95}$$

$$\mathrm{i}\partial_t \chi = kV_y\chi + k\phi, \tag{96}$$

where we have introduced a wave number k in y-direction, and $v_g^2 = \rho_0' g a^2/\rho_0 U^2$ (> 0) and $\Psi = -\Delta\phi$ are the phase velocity of the gravity wave (normalized by U) and vorticity, respectively.

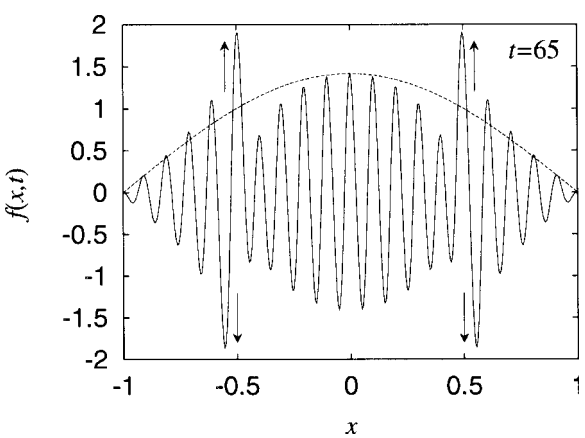

Fig. 11 The vorticity $f(x,t)$ at $t = 65$. The initial condition is $f(x,0) = \sqrt{2}\cos(\pi x/2)$. The amplitude increases near the resonant surfaces $x = \mu_\pm (\simeq \pm 0.495)$.

Because $V_y''(x)$ yields delta functions, the perturbed vorticity Ψ must include delta functions, representing the surface wave perturbations; We write

$$\Psi(x,t) = \alpha_1(t)\delta(x+1) + \alpha_2(t)\delta(x-1) + f(x,t), \tag{97}$$

where $\alpha_1(t)$ and $\alpha_2(t)$ represent the amplitudes of the surface waves and $f(x,t)$ is the continuous part of the vorticity fluctuation. Then, we obtain

$$\mathrm{i}\partial_t f = kxf(x,t) + kV_y''(x)\phi(x,t) + kv_g^2\chi(x,t), \tag{98}$$

$$\mathrm{i}\frac{\mathrm{d}\alpha_1}{\mathrm{d}t} = k\alpha_1(t) + k\phi(-1,t), \tag{99}$$

$$\mathrm{i}\frac{\mathrm{d}\alpha_2}{\mathrm{d}t} = k\alpha_2(t) - k\phi(1,t), \tag{100}$$

$$\mathrm{i}\partial_t\chi = kx\chi(x,t) + kv_g^2\phi(x,t), \tag{101}$$

where

$$\phi(x,t) = K\Psi = \frac{1}{2k}\left(\alpha_1(t)\,\mathrm{e}^{-k|x+1|} + \alpha_2(t)\,\mathrm{e}^{-k|x-1|} + \int_{-\infty}^{+\infty} \mathrm{e}^{-k|x-\xi|} f(\xi,t)\,\mathrm{d}\xi\right), \tag{102}$$

in the infinite domain. Or in the matrix form, we obtian

$$\mathrm{i}\partial_t \begin{pmatrix} f(x) \\ \chi(x) \\ \alpha_1 \\ \alpha_2 \end{pmatrix} = \begin{pmatrix} kx & kv_g^2 & 0 & 0 \\ kK_x & kx & \frac{1}{2}\mathrm{e}^{-k|x+1|} & \frac{1}{2}\mathrm{e}^{-k|x-1|} \\ kK_{-1} & 0 & -\frac{1}{2}(2k-1) & \frac{1}{2}\mathrm{e}^{-2k} \\ -kK_1 & 0 & -\frac{1}{2}\mathrm{e}^{-2k} & \frac{1}{2}(2k-1) \end{pmatrix} \begin{pmatrix} f(x) \\ \chi(x) \\ \alpha_1 \\ \alpha_2 \end{pmatrix}. \tag{103}$$

The equations derived here are exactly equivalent to those in Ref. [11]. Here, we have rederived them from a different set of equations in order to demonstrate that this structure has wide generality.

We rewrite $\lambda_\pm$, $\mu_\pm$ more generally as

$$\lambda_\pm = \pm\frac{1}{2}\sqrt{(2k-1)^2 - \mathrm{e}^{-4k}}, \tag{104}$$

$$\mu_\pm = \pm\frac{1}{2k}\sqrt{(2k-1)^2 - \mathrm{e}^{-4k}}. \tag{105}$$

Observing $f(x)$ at $x = \mu_+$ (or $x = \mu_-$), Eq. (103) reads

$$\mathrm{i}\frac{\mathrm{d}}{\mathrm{d}t}\begin{pmatrix} f(\mu_+) \\ \chi(\mu_+) \\ \alpha_1 \\ \alpha_2 \end{pmatrix} = \begin{pmatrix} k\mu_+ & k\nu_g^2 & 0 & 0 \\ 0 & k\mu_+ & \frac{1}{2}\mathrm{e}^{-k|\mu_+ +1|} & \frac{1}{2}\mathrm{e}^{-k|\mu_+ -1|} \\ 0 & 0 & -\frac{1}{2}(2k-1) & \frac{1}{2}\mathrm{e}^{-2k} \\ 0 & 0 & -\frac{1}{2}\mathrm{e}^{-2k} & \frac{1}{2}(2k-1) \end{pmatrix} \begin{pmatrix} f(\mu_+) \\ \chi(\mu_+) \\ \alpha_1 \\ \alpha_2 \end{pmatrix}. \tag{106}$$

The generator of Eq. (106) can be written in a Jordan canonical form

$$T\begin{pmatrix} \lambda_+ & 1 & 0 & 0 \\ 0 & \lambda_+ & 1 & 0 \\ 0 & 0 & \lambda_+ & 0 \\ 0 & 0 & 0 & \lambda_- \end{pmatrix} T^{-1}, \tag{107}$$

by means of a non-orthogonal transform T. Therefore, we conjecture that $f(\mu_+, t) \propto t^2$ due to the third order degeneracy of the frequency.

However, we observe in Fig. 12 that the asymptotic behavior of $f(\mu_+, t)$ is not proportional to t^2, but $f(\mu_+, t) \propto t$. This is because of the integral terms in Eq. (103), which contribute to the phase mixing damping of the surface waves. The phase mixing damping of the surface wave can be evaluated by renormalizing the perturbative analysis with the assumption $\nu_g^2 \ll 1$ [33]. The renormalized damping rate ν agrees very well with the numerical results.

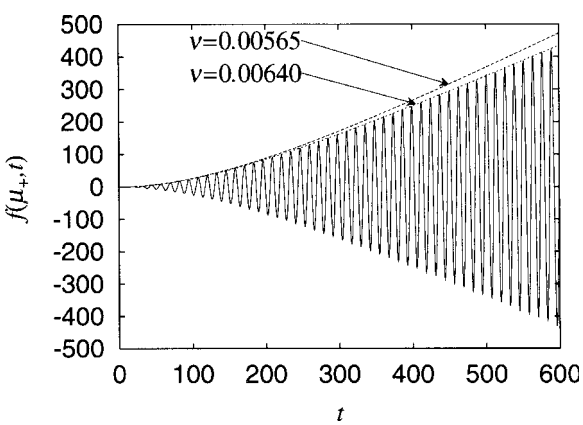

Fig. 12 Time evolution of the vorticity fluctuation $f(x,t)$ at $x = \mu_+$. The amplitude starts to grow in proportion to t^2 and converges to asymptotic growth $\propto t$. Dashed lines denote the analytical fitting curve for a given damping rate ν.

We stress here that such an algebraic instability is not only a mathematical artifact. As we have seen, algebraic growth is observed when the spectra of the Rayleigh equation shows the KH-stable structure [see Fig. 10(b)]. In the infinite domain, KH-unstable (exponential) mode certainly exists for sufficiently small k (see $b = \infty$ case in Fig. 9). However, when a rigid wall is placed close enough ($b \leq 2$ in Figure 9), the spectra of the Rayleigh equation becomes that of Fig. 10(b) for all wave numbers. Thus, we may deduce that there is a system in which algebraic growth dominates the instability.

4. Couette Flow in the Infinite Domain (Kelvin's method)

4.1 Time-dependent eigenmodes

Kelvin's method can resolve, for some classes of mean flows, the evolution of the system

$$\partial_t u + \boldsymbol{V}_0 \cdot \nabla u = A u \tag{108}$$

into new types of modes by means of which both transient and secular asymptotic behaviors are effectively described. Here A denotes a Hermitian differential operator (time-independent) defined in a Hilbert space V, and u ($\in V$) denotes a state vector of the perturbed field. Kelvin's method consists of the combined application of two methods which have been used extensively in the analysis of wave equations. Precisely the "Lagrangian" part of Eq. (108), $\partial_t + \boldsymbol{V}_0 \cdot \nabla$, is solved by means of the characteristics method, and the "Hermitian" part A by means of the standard spectral resolution.

The characteristics method is applied to solve the characteristic ODE associated with the Lagrangian derivative moving along the characteristic curve of the ambient motion, which is given by

$$\frac{\mathrm{d}\boldsymbol{x}}{\mathrm{d}t} = \boldsymbol{V}_0, \quad \boldsymbol{x}(0) = \boldsymbol{\xi}. \tag{109}$$

By inverting the modes, which are denoted in Lagrangian coordinates by $\varphi(\boldsymbol{k}, \boldsymbol{\xi})$, we represent the modes in Eulerian coordinates as

$$\tilde{\varphi}(t;\, \boldsymbol{k},\, \boldsymbol{x}) = \varphi(\boldsymbol{k}, \boldsymbol{\xi}(t;\, \boldsymbol{x})), \tag{110}$$

where $\boldsymbol{\xi}(t;\boldsymbol{x})$ denotes the inverse of $\boldsymbol{x}(t;\boldsymbol{\xi})$. The existence of the inverse mapping $\boldsymbol{x}(t) \rightarrowtail \boldsymbol{\xi}$ is guaranteed in the case of incompressible mean flows. Due to Eq. (110), $\tilde{\varphi}(t;\, \boldsymbol{k},\, \boldsymbol{x})$ satisfies the characteristic equation

$$\partial_t \tilde{\varphi}(t;\boldsymbol{k},\boldsymbol{x}) + \boldsymbol{V}_0 \cdot \nabla \tilde{\varphi}(t;\boldsymbol{k},\boldsymbol{x}) = 0. \qquad (111)$$

The essential condition for the applicability of Kelvin's method consists in the constraint for the functions $\tilde{\varphi}(t;\boldsymbol{k},\boldsymbol{x})$ to form the complete set of eigenfunctions of the operator A [18]. If such a set of eigenfunctions exists, we can decompose the perturbed field u by means of

$$u = \int \hat{u}_k(t)\,\tilde{\varphi}(t;\boldsymbol{k},\boldsymbol{x})\,\mathrm{d}\boldsymbol{k}. \qquad (112)$$

We notice that due to Eq. (110) the eigenvalues of A become time-dependent. The new eigenvalue problem for A reads

$$A\,\tilde{\varphi}(t;\boldsymbol{k},\boldsymbol{x}) = \lambda_k(t)\tilde{\varphi}(t;\boldsymbol{k},\boldsymbol{x}), \qquad (113)$$

where the eigenvalue λ_k also depends on time.

Plugging Eq. (112) into Eq. (108) and exploiting (111) and (113), we obtain

$$\int \left[\partial_t \hat{u}_k(t)\right]\tilde{\varphi}(t;\boldsymbol{k},\boldsymbol{x})\,\mathrm{d}\boldsymbol{k} = \int \hat{u}_k(t)\,\lambda_k(t)\,\tilde{\varphi}(t;\boldsymbol{k},\boldsymbol{x})\,\mathrm{d}\boldsymbol{k}. \qquad (114)$$

Due to the orthogonality of the modes $\tilde{\varphi}(t;\boldsymbol{k},\boldsymbol{x})$, the evolution of $\hat{u}_k$ is governed by the equation

$$\frac{\mathrm{d}}{\mathrm{d}t}\hat{u}_k(t) = \lambda_k(t)\,\hat{u}_k(t). \qquad (115)$$

If $\tilde{\varphi}(t;\boldsymbol{k},\boldsymbol{x})$ do not satisfy both conditions given by characteristic equation (111) and eigenequation (113), then Eq. (114) will have additional terms representing the complicated mode coupling, and thus, the applicability of Kelvin's method is compromised.

The evolution of $\hat{u}_k(t)$ will not exhibit a simple exponential dependence due to the time dependence present in the eigenvalues $\lambda_k(t)$. By analyzing this ODE, we can classify the transient motion and the time asymptotic behavior of each mode.

4.2 Asymptotic and transient behavior

In this section, we show the behavior of Kelvin's mode [time-dependent eigenmode Eq. (110)] for reduced MHD equations (3)–(5). We consider a plasma slab of infinite domain with $V_y(x) = \sigma x$ and $\boldsymbol{B}_0$ = const. The behavior is quite different depending on whether the perturbation is coupled with Alfvén wave or not. Thus, we separately discuss the behavior of the electromagnetic ($\boldsymbol{k}\cdot\boldsymbol{B}_0 \neq 0$) and electrostatic ($\boldsymbol{k}\cdot\boldsymbol{B}_0 = 0$) modes.

4.2.1 Electromagnetic mode

Let us first see the time-asymptotic and transient behavior of electromagnetic mode ($\boldsymbol{k}\cdot\boldsymbol{B}_0 \neq 0$). In the case of $\boldsymbol{B}_0\cdot\nabla \neq 0$, we obtain from Eq. (3)–(5) (see Ref. [12])

$$\left(\partial_t + V_y\,\partial_y\right)\Delta\left(\partial_t + V_y\,\partial_y\right)\psi = \frac{\left(\boldsymbol{B}_0\cdot\nabla\right)^2}{\mu_0\,\rho_0}\Delta\psi - \frac{\rho_0' g}{\rho_0}\,\partial_y^2\,\psi, \qquad (116)$$

where $\Delta = \partial_x^2 + \partial_y^2$ denotes the two-dimensional Laplacian. Since the operator on the right hand side is Hermitian, we can decompose the flux function ψ by means of the shearing eigenmodes [see Eq. (112)]

$$\psi(\boldsymbol{x},t) = \int \hat{\psi}_k(t)\,\tilde{\varphi}(t;\boldsymbol{k},\boldsymbol{x})\,\mathrm{d}\boldsymbol{k}, \qquad (117)$$

where each eigenmode can be expressed by the sinusoidal function

$$\begin{aligned}\tilde{\varphi}(t;\boldsymbol{k},\boldsymbol{x}) &= \exp\left[\mathrm{i}k_x x + \mathrm{i}k_y(y - V_y t) + \mathrm{i}k_z z\right]\\ &= \exp\left[\mathrm{i}\tilde{k}_x(t)x + \mathrm{i}k_y y + \mathrm{i}k_z z\right],\end{aligned} \qquad (118)$$

and $\tilde{k}_x(t) = k_x - k_y\sigma t$. Since Eq. (118) spans the function space V, Eq. (117) gives a complete expansion by means of $\tilde{\varphi}$ [18]. Eigenmodes (118) obeys the governing ODE [see Eq. (115)]

$$\frac{\mathrm{d}^2\hat{\psi}}{\mathrm{d}t^2} + \mu(t)\frac{\mathrm{d}\hat{\psi}}{\mathrm{d}t} + \left[1 - S(t)\right]\hat{\psi} = 0, \qquad (119)$$

where

$$\mu(t) = -\frac{2\sigma k_y\,\tilde{k}_x(t)}{\tilde{k}_x(t)^2 + k_y^2},$$

$$S(t) = -\frac{k_y^2 G}{\tilde{k}_x(t)^2 + k_y^2},$$

and we have omit the subscript k for $\hat{\psi}$. We have normalized the time t by the poloidal Alfvén time $\tau_A = a\sqrt{\mu_0\rho_0}/(\boldsymbol{k}\cdot\boldsymbol{B}_0)$, the wave vector $\boldsymbol{k}$ by the characteristic length scale a, and $\tau_G^2 = -\rho_0/\rho_0' g$ and $G = \tau_A^2/\tau_G^2$. We notice that in the absence of shear flow ($\sigma = 0$) the usual interchange instability equation for static equilibrium can be obtained from Eq. (119) [see Eq. (20)].

When $\sigma \neq 0$, we have $\mu(t) \neq 0$ and we can draw an analogy with the dynamics of a damped oscillator with time-dependent frictional coefficient $\mu(t)$. With time, $\mu(t)$ becomes always positive, which means a formal dissipation, and therefore the oscillation energy of the Alfvén wave $[(\mathrm{d}\hat{\psi}/\mathrm{d}t)^2 + \hat{\psi}^2]/2$ decreases monotonically.

In order to study the time asymptotic behavior, we assume $t \gg k_x/\sigma\,k_y,\ 1/\sigma$. In this limit we obtain the

following ODE;

$$\frac{\mathrm{d}^2}{\mathrm{d}t^2}\hat{\psi} + \frac{2}{t}\frac{\mathrm{d}}{\mathrm{d}t}\hat{\psi} + \left(1 - \frac{G/\sigma^2}{t^2}\right)\hat{\psi} = 0\,, \quad (120)$$

where $G = \tau_A^2/\tau_G^2$ denotes the magnitude of the instability drive term. Since Eq. (120) is the spherical Bessel equation, the time asymptotic behavior of the mode yields

$$\hat{\psi} \sim \frac{1}{t}\sin\left(t - \frac{\pi\nu}{2} + \delta\right), \quad (121)$$

where δ denotes a constant phase depending on the initial conditions. Therefore the mode oscillates with amplitude $\hat{\psi}$ decaying with the inverse power of time. The dependence Eq. (121) corresponds to the similar asymptotic decay in the stream function ϕ, which reads in the leading order as

$$\hat{\phi} \sim \frac{1}{t}\cos\left(t - \frac{\pi\nu}{2} + \delta\right). \quad (122)$$

We note here that there is no threshold value for the stabilization of the interchange instability, since the spherical Bessel equation (120) is common to all modes. Namely, the combined effect of the Alfvén wave propagation and shear flow mixing always overcomes the interchange drive and the oscillations of the magnetic flux asymptotically decay proportional to the inverse power of time.

Since an analytic expression is not available for the transient behavior of each eigenmode, we discuss it by qualitatively analyzing the ODE (119). In the absence of the instability drive, we will have

$$\frac{\mathrm{d}}{\mathrm{d}t}\left[\left(\frac{\mathrm{d}\hat{\psi}}{\mathrm{d}t}\right)^2 + \hat{\psi}^2\right] = -\mu(t)\left(\frac{\mathrm{d}\hat{\psi}}{\mathrm{d}t}\right)^2. \quad (123)$$

Since the sign of the denominator in $\mu(t)$ is always positive, its behavior will be determined by that of the numerator. The numerator is written as $2\sigma^2 k_y^2 t - 2\sigma k_y k_x$ and according to its initial value we can single out two classes of the transients.

When the product $\sigma k_y k_x$ is negative, the frictional coefficient $\mu(t)$ is always positive from the beginning; therefore, the shear flow acts as a damping force at any time and the mode shows simple damped behavior. On the other hand, if the product $\sigma k_y k_x$ is positive, the frictional coefficient $\mu(t)$ is initially negative and changes its sign at the instant $t_* = k_x/\sigma k_y$. Therefore the mode experiences an initial amplification lasting until the time t_*, which is even faster than it would be in the presence of only the interchange drive.

4.2.2 Electrostatic mode

When the wave vector is purely perpendicular to the ambient magnetic field ($\boldsymbol{k} \cdot \boldsymbol{B}_0 = 0$), the flux function ψ decouples from ρ and ϕ. From Eqs. (3)–(4), the dynamics of the stream function is governed by

$$\left(\partial_t + V_y\,\partial_y\right)^2 \Delta\phi = -\frac{\rho_0' g}{\rho_0}\,\partial_y^2\phi\,. \quad (124)$$

When we represent ϕ in terms of the shearing mode given in Eq. (118), we obtain the ODE

$$\frac{\mathrm{d}^2}{\mathrm{d}t^2}\left[\left(\tilde{k}_x(t)^2 + k_y^2\right)\hat{\phi}\right] = k_y^2\gamma_G^2\hat{\phi}\,, \quad (125)$$

where $\gamma_G^2 = -\rho_0' g/\rho_0 (= \tau_G^{-2})$ denotes the characteristic growth rate of the interchange instability. Here we have dropped the subscript k for the sake of simplicity. In order to investigate the asymptotic time behavior of each mode, we again assume $t \gg k_x/k_y\sigma$ and $t \gg 1/\sigma$. Then Eq. (125) becomes

$$\frac{\mathrm{d}^2}{\mathrm{d}t^2}\hat{\phi} + \frac{4}{t}\frac{\mathrm{d}}{\mathrm{d}t}\hat{\phi} + \frac{2-\alpha}{t^2}\hat{\phi} = 0\,, \quad (126)$$

where $\alpha = \gamma_G^2/\sigma^2$ denotes the ratio between the interchange destabilizing effect and the flow shear stabilizing one (Richardson number). The general solution of Eq. (126) is

$$\hat{\phi} = C_1 t^{m_+} + C_2 t^{m_-} \quad (127)$$

where

$$m_\pm = \frac{-3 \pm \sqrt{1+4\alpha}}{2}\,. \quad (128)$$

The asymptotic time behavior is therefore dominated by the larger index m_+. Thus we can state the condition for the boundedness of $\tilde{\phi}$ as

$$\alpha \le 2 \;\Rightarrow\; -\frac{1}{2}\frac{\rho_0' g}{\rho_0} \le \sigma^2\,. \quad (129)$$

The condition for the boundedness of $\tilde{\phi}$ is improved compared with the static case ($\rho_0' \ge 0$) due to the stretching effect of the shear flow. The electrostatic ($\boldsymbol{k} \cdot \boldsymbol{B}_0 = 0$) mode can be linearly unstable while the electromagnetic ($\boldsymbol{k} \cdot \boldsymbol{B}_0 \neq 0$) mode is completely stabilized [see (121) and (122)]. However, the asymptotic behavior is algebraic in time.

5. Couette Flow in the Finite Domain

5.1 Perturbative analysis of eigenvalues

We consider a finite domain $[-a, a]$ in this section with a linear flow such as (see also Fig. 13)

$$V_y(x) = \sigma x, \tag{130}$$

where the shear parameter σ is a real constant. The conventional KH instability is absent because $V_y'' = 0$ [3,14]. Transforming $\partial_t \to -i\omega$ and $\nabla \to i\boldsymbol{k}$, we obtain

$$\frac{d^2\phi}{dx^2} - k_y^2\phi - \frac{2k_y\sigma k_\parallel^2}{\Omega^2\left(\Omega^2 - k_\parallel^2\right)}\left(k_y\sigma\phi + \Omega\frac{d\phi}{dx}\right) - \frac{k_y^2 G}{\Omega^2 - k_\parallel^2}\phi = 0\,. \tag{131}$$

under the normalization in terms of the Alfvén velocity $v_A = B_0/\sqrt{\mu_0\rho_0}$ and the system size a, where $\Omega = \omega - k_y V_y(x)$ is the Doppler shifted local frequency.

We now assume $\sigma \ll 1$ and represent a perturbative analysis for the ODE (131). We expand eigenfunctions and eigenvalues as

$$\phi = \phi_0 + \phi_1 + \phi_2 + \cdots, \quad \omega = \omega_0 + \omega_1 + \omega_2 + \cdots, \tag{132}$$

where $|\omega_n|/|\omega_0| \sim |\phi_n|/|\phi_0| \sim O(\sigma^n)$. From the $O(1)$ terms, we obtain

$$\frac{d^2\phi_0}{dx^2} - k_y^2\left(1 + \frac{G}{\omega_0^2 - k_\parallel^2}\right)\phi_0 = 0\,, \tag{133}$$

which has been already solved in Sec. **2.3**. Eigenvalues and eigenfunctions are

$$\left(\omega_0^{(n)}\right)^2 = k_\parallel^2 - \frac{k_y^2 G}{k_y^2 + n^2\pi^2/4}\,, \tag{134}$$

and

$$\phi_0^{(n)} = \begin{cases} \cos(n\pi x/2) & \text{for } n\text{: odd} \\ \sin(n\pi x/2) & \text{for } n\text{: even} \end{cases}, \tag{135}$$

respectively. We study the effect of the shear flow for the mode $n = 1$, which is the most unstable when $\boldsymbol{V}_0 = \boldsymbol{0}$.

The terms of $O(\sigma)$ yields

$$\frac{d^2\phi_1}{dx^2} - k_y^2\left(1 + \frac{G}{\omega_0^2 - k_\parallel^2}\right)\phi_1 - \frac{2k_y k_\parallel^2\sigma}{\omega_0\left(\omega_0^2 - k_\parallel^2\right)}\frac{d\phi_0}{dx} + \frac{2\omega_0 k_y^2 G}{\left(\omega_0^2 - k_\parallel^2\right)^2}\left(\omega_1 - k_y\sigma x\right)\phi_0 = 0\,. \tag{136}$$

Multiplying $\phi_0^{(1)}$ on both sides of Eq. (136) and integrating it over the domain, we find

$$\omega_1 = 0. \tag{137}$$

The next order equation, thus, describes the effect of the flow shear on the eigenvalue.

After the tedious but straightforward calculation due to the expansion of ϕ_1 in terms of $\phi_0^{(n)}$, we finally obtain the second order dispersion relation (see Ref. [13])

$$2\omega_0\omega_2 = -\frac{k_\parallel^2\sigma^2}{G}\left(1 + 4P_{4+}B + \frac{16}{\pi^2}P_{4+}^2 A\right) + k_y^2\sigma^2\left(\frac{16}{\pi^6}P_{4+}A + 3B\right), \tag{138}$$

where

$$A = \sum_{m=1}^{\infty}\frac{m^2}{\left(m^2 - 1/4\right)^5} \simeq 4.219581\,, \tag{139}$$

$$B = \frac{1}{3} - \frac{2}{\pi^2} \simeq 0.130691\,, \tag{140}$$

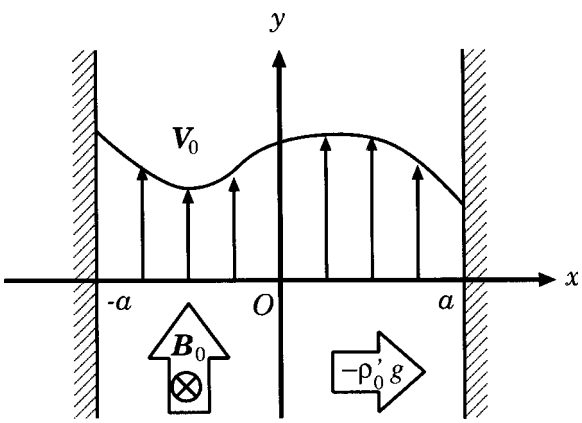

Fig. 13 Slab geometry with gravity.

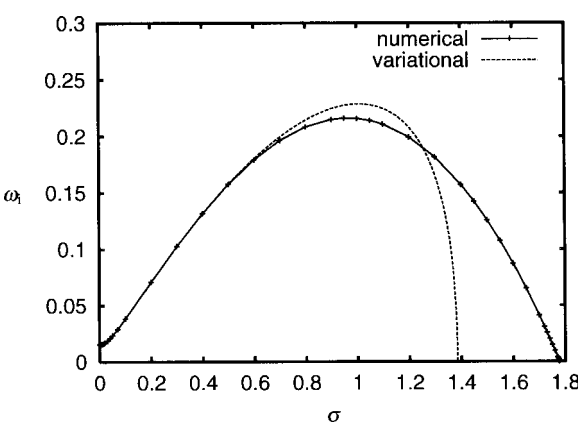

Fig. 14 The growth as a function of the shear parameter σ ($G = 2.72$ and $k_y = k_\parallel = 0.5$). Numerical results are obtained from the direct solution to the eigenvalue problem Eq. (131) by the shooting method.

$$P_{4+} = k_y^2 + \frac{\pi^2}{4}. \tag{141}$$

When ω_0 describes instability (pure imaginary with $\mathrm{Im}\,\omega_0 > 0$), the first term on the right hand side of Eq. (138) brings about a destabilizing effect, while the second causes a stabilizing effect. The destabilizing term contains both $k_\parallel$ and G, while the stabilizing one contains only k_y. It is remarkable that $k_\parallel^2$ works to increase the growth rate, and G, decreases it, which is opposite to the conventional understandings for static equilibrium. For $k_\parallel = 0$ (or for a neutral fluid), this destabilizing effect does not work. There is a threshold in the ratio of $k_\parallel^2$ and G, where the coefficient of σ^2 changes its sign.

Variational calculation yields the maximum growth rate with respect to the local maximum flow velocity $V_{\max} = \sigma$

$$V_{\max} \sim \frac{k_\parallel^2 v_A}{k_y} = \frac{\omega_A}{k_y}, \tag{142}$$

where ω_A is the Alfvén frequency. Over this critical velocity (or σ), the growth rate starts to diminish, implying the onset of the shear flow stretching effect.

5.2 Discussion

Shear flows may stabilize instabilities when they stretch the fluctuation. However, the condition (142) shows that the stabilization occurs only if the local velocity exceeds the phase velocity of the Alfvén wave. When the flow shear is weak, modes may be even destabilized; the growth rate achieves a maximum value, as a function of the maximum flow velocity, near the Alfvén velocity [see Eq. (142)], and it is then suppressed due to the stretching effect overcoming the Alfvénic phase propagation against the flow. We note that this situation is very different when we consider a mathematical model of infinite-domain linear shear flow (Sec. **4**). For such a model, the maximum velocity is unbounded, and hence, we see only the stabilization of instabilities [12].

Let us see how some interchange modes are destabilized in a weak shear flow. Under the incompressibility condition, the energy balance in the perturbed field reads [see also Eq. (6)]

$$\frac{\mathrm{d}}{\mathrm{d}t}\int \frac{1}{2}\rho_0 v^2 + \frac{1}{2\mu_0} b^2 + \frac{g}{2\rho_0'}\rho_1^2\,\mathrm{d}\boldsymbol{v} = \int -\rho_0 V_y' v_x v_y + \frac{V_y'}{\mu_0} b_x b_y\,\mathrm{d}\boldsymbol{v}. \tag{143}$$

where $v^2 = v_x^2 + v_y^2$ and $b^2 = b_x^2 + b_y^2$. In the case of a static equilibrium ($V_y = 0$), the eigenfunctions determined by Eq. (20) are real functions. Then, we obtain mirror symmetric streamlines, which leads to the exact cancellation of the $v_x v_y$ term when integrated. However, an ambient shear flow ($V_y' \neq 0$) yields the complex-valued eigenfunction ϕ, where the integral of $v_x v_y$ remains finite because of the breakdown of the symmetry. Figure 15 shows the streamlines of the eigenfunction for the cases $\sigma = 0.7$ and 1.5. We observe that the product $v_x v_y$ has negative value in most of the domain, if $\sigma = 0.7$. Since $V_y' = \sigma$ is a positive constant, this term (representing the work done by the shear flow) gives a positive contribution in the right hand side of Eq. (143). It is remarkable that the stream line contour is inclined in the opposite direction to the ambient shear flow. The mode corresponding to the complex conjugate eigenvalue (damping mode) has the opposite structure — the streamlines are distorted in the direction of the flow. As σ increases, the ambient flow begins to distort the mode to the direction of the flow, and finally stabilizes it.

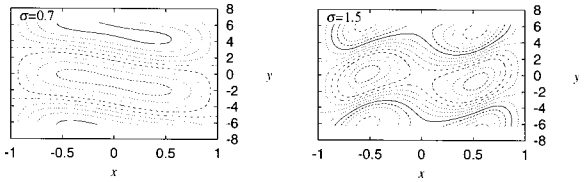

Fig. 15 Streamlines of the typical eigenfunction. The parameters are $B_z = 0$, $G = 2.72$, $k_\parallel = k_y = 0.5$, and $\sigma = 0.7$, and 1.5.

6. Summary

We have reviewed recent studies for constructing a linear stability theory of shear flow plasmas from the viewpoint of spectral analysis. Mathematically, the non-Hermiticity of the operator due to shear flow does not only imply complex eigenvalues, but also the incompleteness of spectral resolution. Physically, shear flow not only has a stabilizing effect due to its stretching mechanism, but also has a destabilizing effect by causing the mode for stationary standing structure in the face of an ambient wave.

We first revisited Rayleigh's analysis of Kelvin-Helmholtz instability for a piece-wise linear shear flow profile and clarified the necessity of nonzero V_y'' for instability. The term containing V_y'' carries the surface wave which supports the mode's stationary structure. Eigenvalue analysis of the Rayleigh equation indicates the overlap of frequency spectra (nilpotent). This yields,

when we include the density gradient (gravity wave), the secular growth of vorticity in time (Sec. **3**).

Kelvin's modal approach is a particular form of generalized spectral method to obtain a general solution of the system; however, it is restricted to a particular shear flow profile. According to this analysis, all modes show asymptotically algebraic behavior in time (Sec. **4**). When we consider a finite domain by imposing a conducting wall, we observe a destabilizing effect of shear flow in the presence of the Alfvén wave (Sec. **5**).

Many unresolved questions remain:

1. When we fix the flow profile and focus on the field line bending effect, it affects the destabilizing mechanism for finite domain Couette flow [see Eq. (138)], while it also affects stabilizing in the infinite domain [see Eqs. (122) and (127)].
2. Rayleigh's criterion insists V_y'' must change its sign in the domain. We found here that nonzero V_y'' is responsible for the stationary structure of the mode; however, we still do not know why it must change its sign. A complete physical understanding of this phenomenon has not been achieved.
3. Is resonance between continua universal over the different sources? For example, does similar secularity happen if Alfvén and flow continua are in resonance?
4. It is obvious that exponential is not the only dependence of instability for non-Hermitian operators. How rich in variety do the linear asymptotic behavior show for them?

When we consider multidimensional equilibrium, more and more questions come to mind. Even area-occupied spectra are observed for non-Hermitian operators [34,35]. We still do not know if we may dream of the possibility of spectral resolution for a non-Hermitian operator, or if we may prove any necessary and sufficient condition for stability such as an energy principle for static equilibria. These questions are left to be answered in the future.

References

[1] S. Chandrasekhar, *Hydrodynamic and Hydromagnetic Stability* (Clarendon, Oxford, 1961).

[2] G.K. Batchelor, *An Introduction to Fluid Dynamics* (Cambridge Univ., Cambridge, 1967).

[3] P.G. Drazin and W.H. Reid, *Hydrodynamic Stability* (Cambridge Univ., Cambridge, 1981).

[4] L.N. Trefethen *et al.*, Science **261**, 578 (1993); P.J. Schmid, Phys. Plasmas **7**, 1788 (2000).

[5] I.B. Bernstein *et al.*, Proc. R. Soc. London, Ser. A **244**, 17 (1958).

[6] J.P. Freidberg, *Ideal Magnetohydrodynamics* (Plenum, New York, 1987).

[7] A.E. Lifschitz, *Magnetohydrodynamics and Spectral Theory* (Kluwer, Dordrecht, 1989).

[8] K. Yosida, *Functional Analysis*, (Springer Verlag, Berlin, 1995).

[9] P.D. Lax, *Functional Analysis* (Wiley, New York, 2002).

[10] Z. Yoshida, *Hisenkei Kagaku Nyumon* (Iwanami, Tokyo, 1998) [*in Japanese*].

[11] M. Hirota, T. Tatsuno, S. Kondoh and Z. Yoshida, Phys. Plasmas **9**, 1177 (2002).

[12] T. Tatsuno, F. Volponi and Z. Yoshida, Phys. Plasmas **8**, 399 (2001).

[13] T. Tatsuno, Z. Yoshida and S.M. Mahajan, Phys. Plasmas, **10**, 2278 (2003).

[14] J.W.S. Rayleigh, Proc. London Math. Soc. **9**, 57 (1880).

[15] W. Thomson (Lord Kelvin), Philos. Mag., Ser. 5 **24**, 188 (1887).

[16] W.O. Criminale and P.G. Drazin, Stud. Appl. Math. **83**, 123 (1990); G.D. Chagelishvili, A.D. Rogava and I.N. Segal, Phys. Rev. E **50**, 4283 (1994); A.D. Rogava and S.M. Mahajan, Phys. Rev. E **55**, 1185 (1997).

[17] F. Volponi, Z. Yoshida and T. Tatsuno, Phys. Plasmas **7**, 2314 (2000).

[18] F. Volponi and Z. Yoshida, J. Phys. Soc. Japan **71**, 1870 (2002).

[19] H.R. Strauss, Phys. Fluids **19**, 134 (1976).

[20] H.R. Strauss, Phys. Fluids **20**, 1354 (1977).

[21] T. Tatsuno, PhD thesis, Kyoto University (2002).

[22] J. von Neumann, *Mathematical Foundation of Quantum Mechanics* (Princeton Univ., Princeton, 1996).

[23] G. Laval, C. Mercier and R.M. Pellat, Nucl. Fusion **5**, 156 (1965).

[24] E.A. Coddington and N. Levinson, *Theory of Ordinary Differential Equations* (McGraw-Hill, New York, 1955).

[25] E.L. Ince, *Ordinary Differential Equations* (Dover, New York, 1956).

[26] Z. Yoshida, *Shudan Gensho no Suri* (Iwanami, Tokyo, 1995) [*in Japanese*].

[27] J.A. Tataronis, J. Plasma Phys. **13**, 87 (1975).

[28] W.A. Newcomb, Ann. Phys. **10**, 232 (1960).

[29] J.P. Goedbloed and P.H. Sakanaka, Phys. Fluids

17, 908 (1974).
[30] K. Appert, R. Gruber, F. Troyon and J. Vaclavik, Plasma Phys. **24**, 1147 (1982).
[31] R.C. Davidson, *Physics of Nonneutral Plasmas* (Addison-Wesley, Redwood, 1990).
[32] S. Kondoh, T. Tatsuno and Z. Yoshida, Phys. Plasmas **8**, 2635 (2001).
[33] M. Hirota, T. Tatsuno and Z. Yoshida, J. Plasma Phys. **69**, 397 (2003).
[34] Z. Yoshida and Y. Giga, Math. Z. **204**, 235 (1990).
[35] A. Lifschitz, Phys. Fluids **9**, 2864 (1997).